ACS SENSORS

pubs.acs.org/acssensors Article

Engineering Bacteria to Monitor the Bleeding of Animals Using Far-Red Fluorescence

Zi-Zhu Tan, Xiao-Dan Li, Chao-Di Kong, Na Sha, Ya-Nan Hou, and Kai-Hong Zhao*

Cite This: *ACS Sens.* 2021, 6, 1770–1778 Read Online

ACCESS | Metrics & More | Article Recommendations | Supporting Information

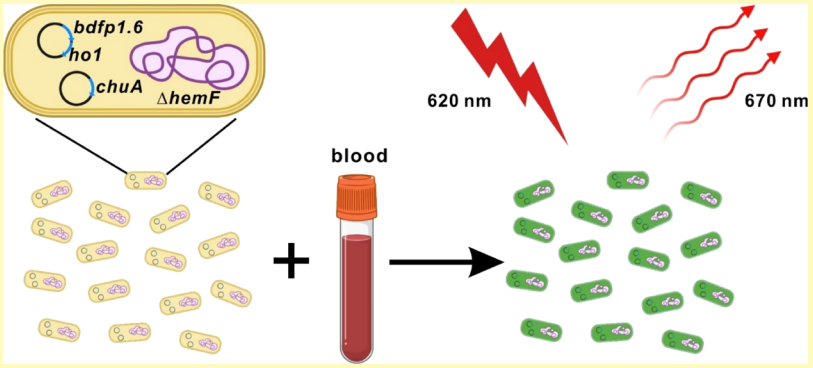

ABSTRACT: Microorganisms living in animals can function as drug delivery systems or as detectors for some diseases. Here, we developed a biosensor constructed by the deletion of *hemF* and harboring *ho1*, *chuA*, and *bdfp*1.6 in *Escherichia coli*. HemF is an enzyme involved in heme synthesis in *E. coli*. ChuA and HO1 can transfer extracellular heme into cells and generate biliverdin (BV). BDFP1.6 can bind BV autocatalytically, and it emits a far-red fluorescence signal at 667 nm. Therefore, we named this biosensor as the far-red light for bleeding detector (FRLBD). Our results indicated that the FRLBD was highly efficient and specific for detecting heme or blood in vitro. Moreover, the FRLBD could be used to detect bleeding in the zebrafish induced by aspirin, and a convolutional neural network was an appropriate model to identify the fluorescence features in the images.

KEYWORDS: *engineering bacteria, far-red light, phycobiliprotein, BDFP, heme, biliverdin*

Microorganisms living in animals affect human health and have been used to detect or treat some diseases.[1−4] Recently, synthetic microbes producing and delivering therapeutics have been found to have broad applications in human diseases.[1] Engineered bacteria can be used to accelerate disease diagnoses. They can recognize an input signal related to some diseases and generate output signals, such as fluorescence, luminescence, and enzymatic activity.[5−8] Additionally, it is necessary for researchers to optimize a specific, sensitive, reliable, and robust gene circle to respond to the input signals and to produce the output signals. Synthetic biology is an effective method to construct these gene circles that control gene expression with small molecular compounds or proteins, which can function as transcription factors (TFs) to activate or inactivate reporter gene expression.[1] Moreover, bacterial two-component systems (TCSs) comprised a sensor kinase and a response regulator provide tremendous potential for such biosensors.[9] However, due to the system diversity and heterologous expression of reporter genes or the transference of promoters and TFs to heterologous systems, TF/promoter biosensors may present challenges for specificity.[10] Even so, TF-based biosensors still have potential applications in the detection of intestinal diseases.[5,11]

In the past, wireless capsule endoscopy equipped with a small camera was the primary technology for detecting diseases in the gut. It took pictures in different parts of the intestinal tract, relying on the movement of the gut to transport it, and then, it transmitted the pictures to a computer. After that, the huge number of pictures was analyzed through machine learning, for example, neural networks or support vector machines, to determine the severity of the bleeding in the gut.[12−14] However, wireless capsule endoscopy equipped with a camera might not obtain accurate pathological imaging since it is completely dependent on the movement of the gut. Therefore, to overcome these shortcomings, some researchers tried transmitting fluorescent signals, not pictures, to the computer using wireless capsule endoscopy equipped with a small fluoroscopy device to detect any blood in the gut.[15] This

Received: November 27, 2020
Accepted: April 28, 2021
Published: May 12, 2021

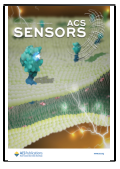

https://doi.org/10.1021/acssensors.0c02482
ACS Sens. 2021, 6, 1770–1778

method avoided the time-consuming, tedious analysis of pictures and provided an efficient strategy for the real-time detection of gastrointestinal bleeding, but it was necessary to inject a fluorescent dye into the patient's bloodstream before performing the capsule endoscopy. Recently, TF-based biosensors, which could respond to heme, were created as engineered bacteria designed to detect blood. Therefore, wireless capsule endoscopy equipped with such a biosensor could function as a detector for bleeding in the intestinal tract.[11] As we discussed above, such biosensors present challenges for specificity.

Genetically encoded green fluorescent proteins (FPs)[16] and their variants have been widely used in biolabeling,[17] protein−protein interactions,[18] and biosensors for pH,[19] Ca^{2+},[20] and cell cycle features.[21] Far-red (FR) and near-infrared (NIR) (from 650 to 900 nm) FPs derived from bacteriophytochromes (Bphys)[22] and phycobiliproteins (PBPs)[23] broaden the spectral range of FPs and have noninvasive and deep tissue imaging characteristics.[24] They both need to bind to biliverdin (BV) to fluoresce, and BV is widely distributed in animals but not in *Escherichia coli*.

Far-red (FR) and near-infrared (NIR) FPs require BV to fluoresce. In this work, we hoped to integrate this process into engineered bacteria and provided a new strategy for the detection of heme, which can be oxidized by heme oxygenase-1 (HO1), yielding equimolar quantities of carbon monoxide, iron ions, and BV.[25] This strategy was not based on the TF but instead on the enzyme reaction. Our data showed that it was an efficient, sensitive, and specific method for the detection of blood in vitro. Furthermore, our method could use FR fluorescence as the output signal. This makes it possible to use our biosensor to detect bleeding in deep tissues through imaging, such as in the intestinal tract. Additionally, FR fluorescence is important for gastrointestinal diagnosis using capsule endoscopy.[26]

MATERIALS AND METHODS

Plasmid Construction. Standard protocols were used to perform the genetic manipulations.[27] DNA coding ChuA was synthesized (Tianyi Huiyuan Biotech Company, China). Then, it was cloned into pACYCDuet using the *Nco*I and *Xho*I restriction sites, which had chloramphenicol resistance, and *ho1* and *bdfp1.6* were PCR-amplified from the previously constructed pACYCDuet-ho1[28] and pET28a-bdfp1.6,[29] respectively. Then, *ho1* was cloned into the first open reading frames (ORFs) of pCDFDuet using *Nco*I and *Pst*I, and *bdfp1.6* was cloned into the second ORFs using *Bgl*II and *Xho*I. pCDFDuet-ho1-bdfp1.6 is resistant to streptomycin.

Deletion of *hemF* in *E. coli*. pKD4, a plasmid with kanamycin resistance and FRT sites, was used as the template to amplify the flanking regions of the *hemF*, kanamycin gene, and FRT sites. pKD46, a plasmid with ampicillin resistance, λ red recombinase, and an arabinose promoter, was transformed into *E. coli* strain BL21. Luria−Bertani (LB) medium with ampicillin (50 μg/mL) was used to culture the *E. coli* containing pKD46. When the OD_{600} was 0.2−0.3, 2% arabinose was used to induce the expression of λ red recombinase. After that, the fragments with flanking regions of the *hemF*, kanamycin gene, and FRT sites were transformed into *E. coli* containing λ red recombinase. Successful recombinant strains were screened for growth on LB plates containing kanamycin (30 μg/mL) and verified by PCR. To remove the pKD46 plasmid, the recombinant strains were grown overnight at 42 °C.

Protein Expression. BDFP1.6 and HO1 were coexpressed with ChuA using terrific broth medium containing kanamycin (30 μg/mL), chloramphenicol (40 μg/mL), and streptomycin (50 μg/mL) in *E. coli* BL21 cells. When the OD_{600} of *E. coli* was 0.6−0.8, 1 mM isopropyl β-D-thiogalactoside (IPTG) was used to induce protein expression for 14−16 h at 16 °C, and the cells were centrifuged at 3000*g* for 5 min at 16 °C using a 50 mL centrifuge tube and washed twice with distilled water. To determine whether the biosensor can respond to heme, hemoglobin, or blood, heme (20 μM), hemoglobin (10 μM), and blood (1000 ppm) were added to the medium with IPTG, respectively. After induction for 14−16 h at 16 °C, a fluorescence spectrometer was used to detect the fluorescence of *E. coli*.

Spectral Analysis. The absorption spectra of BDFP1.6 and OD_{600} of *E. coli* were measured using a UV-9000S (Shanghai Metash Instruments Co., Ltd.). The fluorescent spectra were recorded using a model F320 spectrofluorometer (TianJin GangDong Sci and Tech Development Company, China) with excitation at 600 nm and emission at 620 nm.

Protein concentrations were obtained by measuring the absorbance at 280 nm. The molar extinction coefficient of BDFP1.6 at 280 nm was predicted to be 17,460 mol^{-1} cm^{-1} (https://web.expasy.org/protparam/).

Reaction Kinetics and Affinity of FRLBD Responding to Heme or Blood. Heme was dissolved in 100 mM $NaHCO_3$ solution. Blood was obtained from adult female ducks. EDTA (1.5 mg/mL) was added to the blood to prevent clotting, and then, it was stored at 4 °C. Hemoglobin and albumin were dissolved in 20 mM KPB (pH = 7.2). BV was dissolved in DMSO.

Then, 10 μM heme, 1000 ppm blood, buffer, or 10 μM BV was added to the respective engineered *E. coli* induced by IPTG for 14−16 h at 16 °C. The fluorescence was then monitored every 20 min at 37 °C. $t_{1/2}$ was calculated as the time to increase to 50% fluorescence.

For the determination of EC_{50} of the far-red light for bleeding detector (FRLBD)-binding heme, hemoglobin, or blood, the FRLBDs were titrated with different heme, hemoglobin, or blood concentrations (4 h). The fluorescence dependent on the dose could be fitted and processed with a single-site binding model of the Scatchard equation: $F = (F_{max}[c])/(EC_{50} + [c])$, where "$F$" denotes the fluorescence, "$[c]$" denotes the concentration of heme, hemoglobin, or blood, and EC_{50} denotes the 50% effective concentration.

Determination of Heme and Hemoglobin Concentrations in Blood. Standards for hemoglobin, heme, and bilirubin (BR) were prepared in KPB buffer (pH = 7.2), and absorbance between 190 and 800 nm was measured by UV-9000S (Shanghai Metash Instruments Co., Ltd.) at room temperature. Spectra were analyzed by deconvolution algorithms with multiple linear regressions fitting (Python) as described.[30]

Zebrafish Husbandry and Injection. Zebrafish of strain AB were purchased from the Hydrobiology Institute of the Chinese Academy of Sciences and raised at 28 °C with a light cycle of 14 h of light and 10 h of darkness. Chirocephalus was used to feed the zebrafish.

The FRLBD *E. coli* was induced by IPTG at 16 °C to express BDFP1.6, HO1, and ChuA for 16 h. After that, the cells were centrifuged at 3000*g* for 5 min at 16 °C using a 50 mL centrifuge tube and washed twice with distilled water. To determine whether the FRLBD can detect bleeding in the zebrafish, zebrafish were anesthetized using 3-aminobenzoic acid ethyl ester methanesulfonate (MS-222, 100 mg/L). The FRLBD (4×10^6 cfu) was injected into the zebrafish abdomen using a microinjector. After four days, 10 μL of water or aspirin (20 mg/mL)[31] was injected into the abdomen using the same method. Considering the insolubility of aspirin in water, the aspirin was ground into powder and suspended in water. Then, it was injected into the zebrafish. After 4 days, the zebrafish were imaged using a Qipx420 (Molecular Devices Company) with excitation at 628 nm and emission at 692 nm. All experiments using zebrafish were approved by the Scientific Ethics Committee of Huazhong Agricultural University.

Deep Learning. A total of 57 images containing 28 negative images (no bleeding) and 29 positive images (bleeding) were used to construct the convolutional neural network (CNN) models. Among them, two-thirds of the images were used for training the models, and a third of the images were used to test the accuracy of the models.

https://doi.org/10.1021/acssensors.0c02482
ACS Sens. 2021, 6, 1770−1778

The CNN was constructed with Keras (https://keras.io/) using Python3.7.5 (https://www.python.org/).

Quantification and Statistical Analysis. To calculate the mean fluorescence intensity of the engineered *E. coli* in our experiments, three independent biological replicates were conducted to ensure *P* values <0.05 for the majority of significant comparisons. Two-tailed Student's *t*-test was used to calculate the *P* values. All error bars represent the SD (n = 3, number of samples). To determine whether FRLBD can detect bleeding in zebrafish, 20 zebrafish were randomly selected to inject with FRLBD *E. coli* and water, while another 20 zebrafish were injected with FRLBD *E. coli* and aspirin. All fluorescence images were adjusted and analyzed with ImageJ (National Institutes of Health). Graphs and statistics were processed with Origin 9.0 (OriginLab) or R 3.6.1 (https://www.r-project.org/).

RESULTS

Gene Knockout of *hemF* in *E. coli*. Heme is a complex of iron with protoporphyrin IX, and it plays an important role in oxygen transport, electron transfer, and controlling the expression of numerous proteins.[32] It is an essential prosthetic group for the function of many enzymes and transporters, such as hemoglobin, peroxidases, and cytochromes, in all aerobic cells.[33] Heme is synthesized by a series of enzymes in vivo.[33] 5-Aminolevulinic acid (ALA), a nonprotein amino acid, is the first committed intermediate for the synthesis of heme (Figure S1). In the antepenult step of heme biosynthesis, coproporphyrinogen III (COPROGEN) is oxidized, yielding protoporphyrinogen IX (PROTOGEN) by either oxygen-dependent coproporphyrinogen III oxidase (CPO) or oxygen-independent CPO, which is named *hemF*[34] or *hemN*[35] in *E. coli*, respectively (Figure S1).

Binding with BV is necessary for NIR or FR FPs derived from Bphys or PBPs to emit fluorescence.[22,36] We know that heme can be oxidized by heme oxygenase-1 (HO1) to BV. Therefore, we can create a detector for heme by integrating the above two steps into *E. coli*. However, while BV is nonexistent, heme is ubiquitous in *E. coli*. Therefore, we must cut off the biosynthesis of heme in *E. coli*.

As we discussed above, heme is synthesized from 5-ALA by a series of enzymes in *E. coli* (Figure S1). We attempted to block one of the steps in heme biosynthesis. Since heme is essential,[33] deletion of most genes in the heme synthetic pathway led to inviable cells. However, as *E. coli* encodes both O_2-dependent and -independent CPOs, we surmised that knocking out one of the CPOs would lead to viable cells with reduced heme levels. Indeed, by using λ red recombination,[37] a widely used method in bacterial gene deletion, we were only able to obtain the *hemF* deletion mutant and were unable to knockout the genes *hemB, C, D, E, G, H,* and *N* in *E. coli* strain BL21. Deletion of *hemF* did not adversely affect growth and gene expression in *E. coli* (Figure S2), despite the fact that the production of heme was reduced significantly (see below).

Construction of Gene Circles. We recently reported a group of FR and NIR FPs derived from ApcF2, a phycobilisome core subunit of allophycocyanins, from *Chroococcidiopsis thermalis* sp. PCC7203,[38] the substituents of which were termed BDFP1.1−1.9. Some of them emit in the FR region (~670 nm), while the others emit in the NIR region (~710 nm).[23,29,36] BDFPs, derived from ApcF2, can bind BV autocatalytically. Because the autocatalysis of BDFPs binds to BV, it is the basis of the efficiency and specificity of using BDFPs to detect heme. Here, we chose BDFP1.6,[29] which has been shown to be capable of imaging mammalian cells with high brightness and emitting at ~667 nm (Figure S3), as our reporter.

BV can be generated from heme by HO1, but the *ho1* gene is nonexistent in *E. coli* BL21. However, BV is necessary for BDFP1.6 to fluoresce. Therefore, fluorescence as the output signal could be detected when BDFP1.6 was coexpressed with cyanobacterial HO1 in *E. coli* BL21. We also detected the fluorescence of *E. coli* that lacked *hemF* but expressed BDFP1.6 and HO1. As we expected, the fluorescence was very low (Figure 2a).

We have discussed the theory that engineered *E. coli* lacking the *hemF* gene can function as a detector of heme. However, due to the cell wall and plasma membrane, *E. coli* does not have any permeability for heme.[11] The *chuA* gene, a heme transporter discovered from *E. coli* O157:H7, can be used to transport extracellular heme into *E. coli*.[39] Therefore, we thought that the engineered *E. coli* strain BL21 lacking the *hemF* gene but harboring the *chuA*, *ho1*, and *bdfp1.6* genes could be used as the biosensor for heme (Figure 1a).

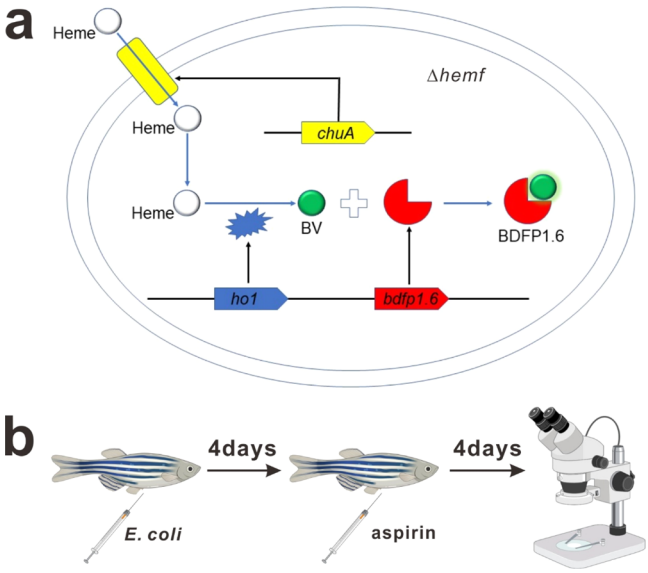

Figure 1. Construction of FRLBD and strategy to detect bleeding in vivo. (a) *E. coli* strain BL21 with a deletion of *hemF* was used to construct FRLBD while harboring *ho1*, *bdfp1.6*, and *chuA*. Blue arrows represent the transformation of heme. (b) Strategy of engineered *E. coli* to detect bleeding in zebrafish. *E. coli* (4×10^6 cfu) was injected into the abdomen of zebrafish using a microinjector. After 4 days, 10 μL of aspirin (20 mg/mL) was injected into the abdomen using the same method. Then, the fluorescence was detected with a fluorescence microscope.

To verify our idea, the three proteins (ChuA, HO1, and BDFP1.6) were coexpressed under the induction of IPTG in *E. coli* with deleted *hemF* at 16 °C. Then, 20 μM heme was added to the medium along with the IPTG. After 14−16 h, we measured the fluorescence intensity of the *E. coli*. Our results showed that the fluorescence of the *E. coli* with heme added was 7.2-fold that without heme addition (Figure 2a). Additionally, we examined the response of *E. coli* without *hemF* deletion and harboring *chuA*, *ho1*, and *bdfp1.6* for heme. To our surprise, instead of increasing the fluorescence, heme reduced the fluorescence intensity of the *E. coli* (Figure 2). Therefore, lack of *hemF* was necessary for *E. coli* to detect the external heme. Our results also indicated that ChuA and HO1

https://doi.org/10.1021/acssensors.0c02482
ACS Sens. 2021, 6, 1770−1778

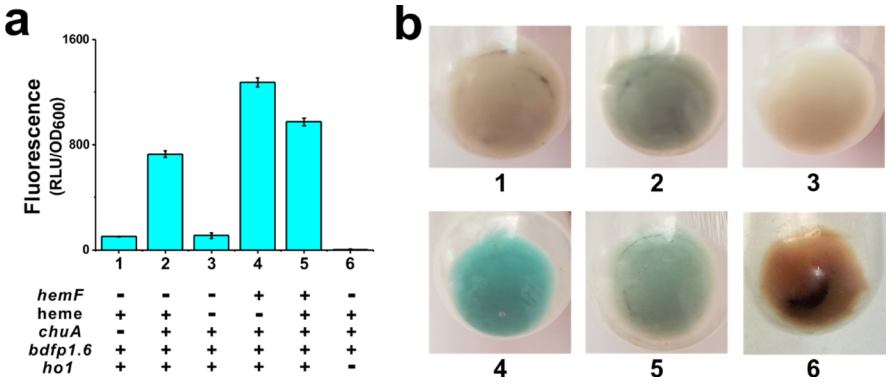

Figure 2. Functional heme biosensing gene circles are necessary for FRLBD detection of heme in vitro. The fluorescence intensity (λ_{ex} = 600 nm, λ_{em} = 620 nm) (a) and cells colors (b) in the engineered *E. coli* with different gene circle or heme addition. *ho1*, *bdfp1.6*, and/or *chuA* were coexpressed in *E. coli* with or without 20 μM heme addition. The *E. coli* with deletion of *hemF* but harboring *ho1*, *chuA*, and *bdfp1.6* are essential for the construction of FRLBD. All data have been subtracted from the background fluorescence of the cells not expressing BDFP1.6. Error bars show standard deviation (n = 3).

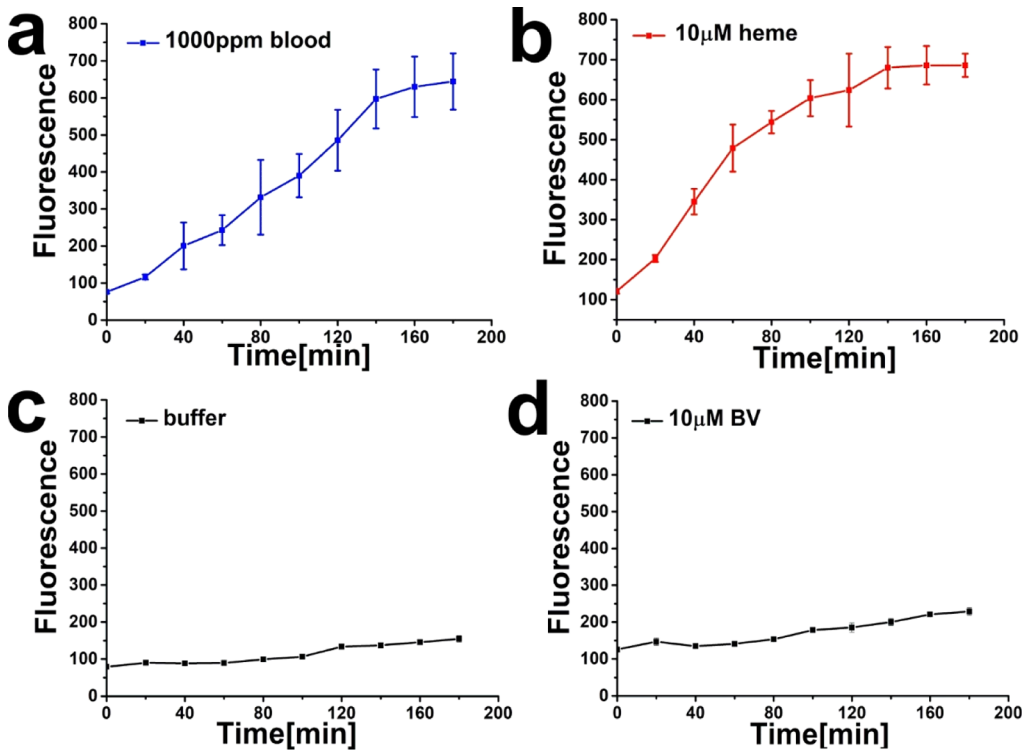

Figure 3. Time-response curves of fluorescence intensity. Engineered *E. coli* lacking *hemF* but expressing HO1, BDFP1.6, and ChuA induced by IPTG for 14−16 h at 16 °C was exposed to 1000 ppm blood (a), 10 μM heme (b), buffer (c), and 10 μM BV (d) at 37 °C. Fluorescence was measured every 20 min. All data have been subtracted from the background fluorescence of the cells not expressing BDFP1.6. Error bars show standard deviation (n = 3).

were necessary for this biosensor to detect heme (Figure 2). To evaluate whether this biosensor can detect blood, we mixed blood (1000 ppm), hemoglobin (10 μM), and albumin (10 μM) with *E. coli* in the same way, respectively. Our results showed that both hemoglobin and blood can activate the fluorescence of this biosensor (Figure S4). Because both heme and hemoglobin in the blood can activate the fluorescence of this sensor, we measured the amount of heme and hemoglobin in plasma (1000 ppm) (Figure S5). We found that the concentration of hemoglobin (3.79 μM) was much greater than the concentration of heme (0.25 μM). Therefore, we thought that the blood activated the fluorescence of this biosensor primarily through hemoglobin (see below).

Reaction between Bacteria with Heme or Blood In Vitro. We have proven that these four elements, Δ*hemF*, *chuA*, *ho1*, and *bdfp1.6*, are essential for *E. coli* to respond to external heme. To confirm the efficiency and specificity of this biosensor in detecting blood or heme, ChuA, HO1, and BDFP1.6 were coexpressed under the control of IPTG for 14−16 h in *E. coli* lacking *hemF* at 16 °C. Then, this biosensor was exposed to 1000 ppm blood or 10 μM heme at 37 °C. After that, we measured the fluorescence intensity every 20 min. After 3 hours, the fluorescence of the *E. coli* reached its maximum and did not increase. Our results indicated that the fluorescence increased by 6- and 8.7-fold, respectively, in the presence of 10 μM heme or 1000 ppm blood (Figure 3a,b).

https://doi.org/10.1021/acssensors.0c02482
ACS Sens. 2021, 6, 1770−1778

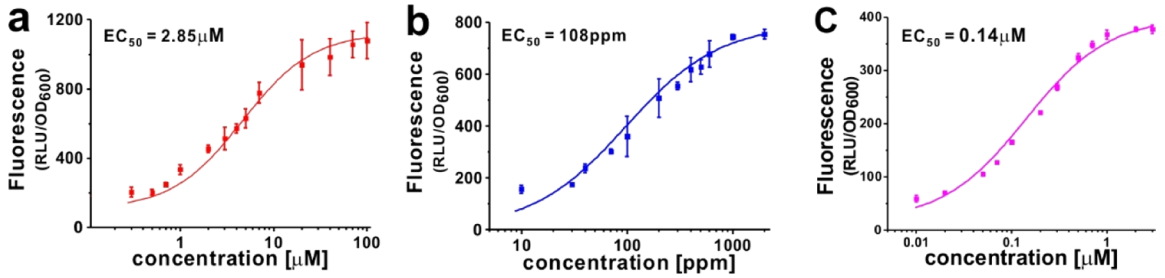

Figure 4. Dose−response curves of fluorescence intensity. Different concentrations of heme (a), blood (b), and hemoglobin (c) were used to induce the fluorescence of FRLBD (4 h). The fluorescence depending on the concentration could be fitted and processed with a single-site binding model of the Scatchard equation: $F = (F_{max}[c])/(EC_{50} + [c])$, where "$F$" denotes the fluorescence, "$[c]$" denotes the concentration, and EC_{50} denotes the 50% effective concentration. All data have been subtracted from the background fluorescence of the cells not expressing BDFP1.6. Error bars show standard deviation (n = 3).

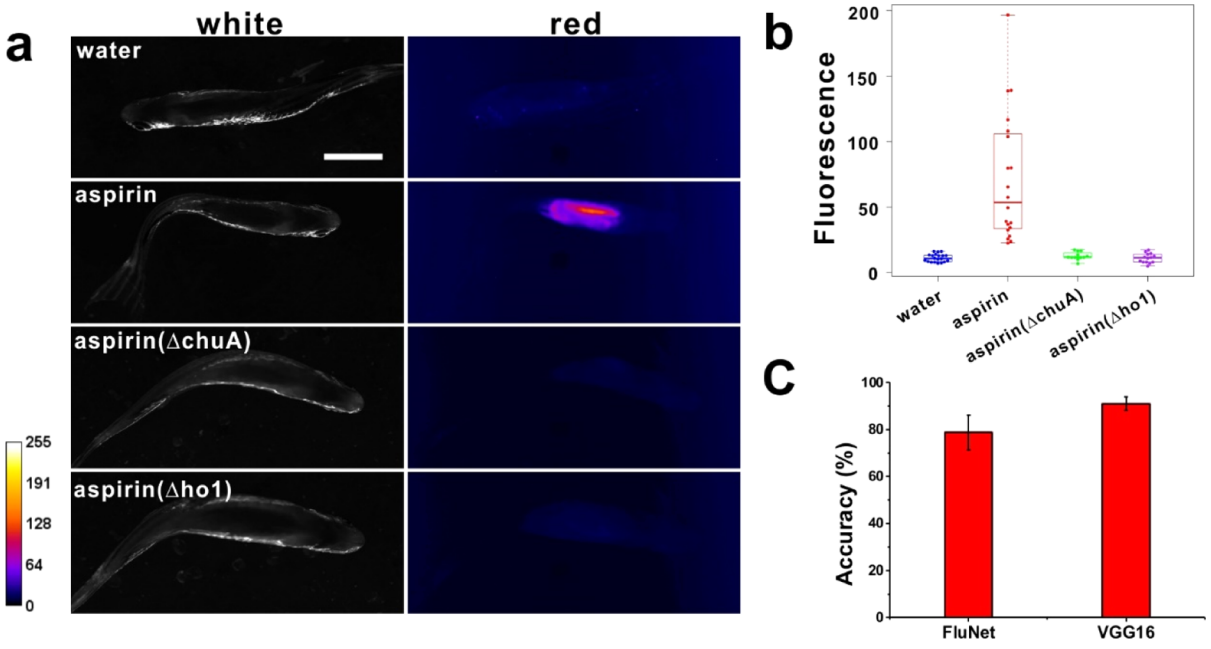

Figure 5. FRLBD detects bleeding in vivo. (a) Fluorescence imaging of zebrafish injected with water or aspirin. FRLBD was used to detect the bleeding induced by aspirin. Left column: zebrafish was observed at the white channel. Right column: zebrafish was imaged at red channel (λ_{ex} = 628 nm and λ_{em} = 692 nm). Fluorescence images were adjusted with ImageJ. Scale bars: 0.5 cm. (b) Fluorescence intensity of the zebrafish abdomen when injecting FRLBD *E. coli* and aspirin or water. Fluorescence intensity was calculated with ImageJ. Normalized fluorescence values of zebrafish were significantly higher in zebrafish injected with aspirin compared to the zebrafish injected with water ($p < 0.01$ two-tailed Student's t-test; N = 20 zebrafish). Moreover, *chuA* and *ho1* were necessary for the detection of bleeding. (c) Accuracy of the CNN model named as FluNet constructed in this paper and VGG16[47] for the recognition of fluorescent images.

Additionally, we calculated the $t_{1/2}$, which was the time required to increase the 50% fluorescence, and they were 48 and 89 min for heme and blood when the engineered *E. coli* was incubated with 10 μM heme or 1000 ppm blood, respectively. We also treated *E. coli* with the same method using heme dissolved in buffer (100 mM $NaHCO_3$) at 37 °C and found that the fluorescence intensity barely increased (Figure 3c). External BV can also activate the fluorescence of BDFP1.6.[40] To determine the specificity of this biosensor for heme, the engineered *E. coli* was exposed to 10 μM BV at 37 °C. We found very little increase in fluorescence caused by BV (Figure 3d). This indicated both the high sensitivity and specificity of the engineered *E. coli* for heme or blood detection. Here, we have reported a biosensor that can detect blood in vitro using FR light, so we named it as the FRLBD.

For the determination of the EC_{50} values of the FRLBD to heme, blood, and hemoglobin, different concentrations of heme, blood, and hemoglobin were used to activate the fluorescence of BDFP1.6 in *E. coli*. The fluorescence showed a concentration dependence. Our results demonstrated that the EC_{50} values were 2.85 μM, 108 ppm, and 0.14 μM for heme, blood, and hemoglobin, respectively (Figure 4).

To determine the optimal reaction conditions between the FRLBD and blood, we measured the fluorescence enhancement of *E. coli* mixed with 1000 ppm blood at different temperatures or pH values. Our results showed that neutral conditions were essential for the reaction of *E. coli* with blood. As we expected, 37 °C was the best reaction temperature in our experiment; the lower the temperature, the slower the enhancement of fluorescence. Such conditions were consistent with the growth of *E. coli*. Therefore, we thought that our biosensor is appropriate for the detection of bleeding in animals.

https://doi.org/10.1021/acssensors.0c02482
ACS Sens. 2021, 6, 1770−1778

Detection of Bleeding in the Zebrafish. As an animal model, zebrafish have been used to widely study pharmacokinetics.[41,42] Here, we used zebrafish to determine whether the FRLBD can detect the bleeding of animals. First, engineered *E. coli* expressing BDFP1.6, ChuA, and HO1 were injected into the abdomen of the zebrafish. After 4 days, water, as the contrast agent, or aspirin, which is an inflammatory drug that can induce gastrointestinal bleeding at high concentrations in humans,[43] were injected into the abdomen using the same method. After 4 days, the zebrafish were imaged under excitation at 628 nm and emission at 692 nm (Figure 1b). Our results demonstrated that the fluorescence of zebrafish injected with aspirin was significantly higher than that of zebrafish injected with water (Figure 5b). Also, ChuA and HO1 were essential for the FRLBD to detect bleeding in zebrafish (Figure 5b).

Deep learning, especially CNNs, has been widely used in the analysis of MR images and tumor diagnosis.[44,45] This method can learn predictive features directly from the images by utilizing a back-propagation algorithm that recalibrates the model's internal parameters after each round of training.[46] This saves much redundant work during image analysis. Therefore, we hoped to use the CNN model to recognize the fluorescent features in the images to identify whether the zebrafish is bleeding. A total of 57 images containing 28 negative images (no bleeding) and 29 positive images (bleeding) were used to verify this approach. Among them, two-thirds of the images were used for training the models, and a third of the images were used to test the accuracy of the models. K-fold cross-validation was used to evaluate the standard deviation of the models. Our results indicated that a simple CNN model containing 4 Conv2D and 4 MaxPooling2D layers showed 78% accuracy in the recognition of fluorescence induced by bleeding, and a complicated model (VGG16) containing 13 Conv2D and 5 MaxPooling2D,[47] a pretrained model, was used as a feature extractor, which showed 91% accuracy (Figure 5c). This result was considered satisfactory; after all, the CNN often requires a lot of data (thousands of images) to show a better accuracy.[48] Therefore, we thought that using the CNN to identify the fluorescent features was a highly feasible method to detect bleeding of the gut or other organs in animals when utilizing FRLBDs.

DISCUSSION

Biosensors based on TF/promoter pairs have been widely used for detecting small molecules, high-throughput screening, and the regulation of gene expression and metabolism in cells.[49,50] Combining optogenetics with a bacterial TCS, researchers have developed biosensors that enable precise control of gene expression using different wavelengths of light.[51,52] Recently, similar biosensors have been used to detect some intestinal diseases, including gut inflammation and bleeding.[5,11] Tetrathionate, which is generated during inflammation, can be detected in these bacteria by the TtrR/TtrS TCS.[53] For the detection of bleeding, a synthetic promoter ($P_{L(HrtO)}$), inactivated by the *Lactococcus lactis* heme-responsive transcriptional repressor HrtR, can be activated by small molecular heme to control the reporter gene expression of *luxCDABE*.[11] However, the limitations of such biosensors are that we cannot guarantee that other factors do not simultaneously activate the promoter. Therefore, TF/promoter biosensors may present challenges for specificity.[10] When these biosensors are used in disease diagnosis or high-throughput screening, false-positive results can be generated from the nonspecificity.[54]

Traditional methods of detecting intestinal bleeding, such as CT, colonoscopy, and capsule endoscopy, can cause a certain degree of injury to the body. They need to take a lot of pictures and spend redundant time to deal with these pictures. In our method, the output signal was produced directly by the reaction of small molecules with proteins or enzymes. Due to the specificity of the enzyme reaction, we thought that this was a feasible strategy to improve the specificity of diagnosis. Our results have shown that the fluorescence signal of BDFP1.6 was related to the blood concentration (Figure 4a). Therefore, we thought that our method is appropriate for reporting the severity of intestinal bleeding. Moreover, the FRLBD uses FR light as the output signal. Considering the penetration and invasiveness of white light, FR light is superior for the noninvasive detection of deep tissues.[26] Recently, infrared fluorescence endoscopy, which is able to detect NIR fluorescence, was created to detect early cancer in the small intestine.[55]

Due to the variability and instantaneity of the mammalian gut, researchers developed genetic memory systems, which comprise a trigger element and a memory element, to recode environmental signals.[56,57] A trigger element can respond to the signals, and a memory element can remember the signals for some time. Recently, researchers have engineered bacteria containing a genetic memory system derived from the cI/Cro region of phage lambda and the TtrR/TtrS TCS. Such a biosensor could retain the memory of gut inflammation for analysis by fecal testing.[5] Therefore, we thought that combining the genetic memory systems with FRLBDs would give a better detector of bleeding in the gut or other organs.

BR is a small molecule associated with important health implications, such as proper liver function.[58] It can be generated from BV by BV reductase.[25] Also, BR can be oxidized to BV by BR oxidase.[25] A low concentration of BR is important for health, but when erythrocytes break down, BR is produced excessively, or glucuronic acid binding is damaged, leading to the disruption of BR metabolism. BR accumulates in the circulation system, and extravascular tissue may result in diseases such as jaundice and kernicterus.[59] We thought that our strategy for the detection of heme was also a feasible idea for the detection of BR.

CONCLUSIONS

Here, we developed a biosensor named FRLBD that could detect bleeding by using small-molecule heme as input signals and FR fluorescence as output signals. In our research, we partially restrained the biosynthesis of heme through the deletion of the *hemF* gene, which is an oxygen-dependent CPO that converts coproporphyrinogen III into protoporphyrinogen IX in the antepenult step of heme biosynthesis. Such a step can also be accomplished by the anaerobic CPO HemN. Because HemN is anaerobic,[35] we thought that oxygen could suppress the biosynthesis of heme. As expected, when BDFP1.6 was coexpressed with HO1 in *E. coli* lacking *hemF*, the fluorescence of BDFP1.6 was very low. We also found that ChuA and HO1 were essential for our engineered bacteria to use extracellular heme to fluoresce. Therefore, *E. coli* with deletion of *hemF* but harboring *ho1*, *chuA*, and *bdfp1.6* can function as a biosensor for heme or blood. Additionally, our results indicated that the FRLBD was highly efficient and specific for the detection of heme. We could detect the bleeding of zebrafish induced by

https://doi.org/10.1021/acssensors.0c02482
ACS Sens. 2021, 6, 1770−1778

aspirin with the FRLBD and identify the fluorescent features in the images through deep learning to determine whether the zebrafish were bleeding. In summary, our study provided a new method for the diagnosis of intestinal bleeding.

■ ASSOCIATED CONTENT

Supporting Information

The Supporting Information is available free of charge at https://pubs.acs.org/doi/10.1021/acssensors.0c02482.

> Engineered *E. coli* can detect and respond_supplement, additional descriptions about the synthesis of heme in *E. coli*, effects of lack of the *hemF* gene on the growth and protein expression of *E. coli*, the spectra of BDFP1.6, blood components and their effects on activation of FRLBD fluorescence, optimal reaction conditions between FRLBD and blood, and models of CNNs and the PCR primers and plasmids for the construction of the gene circle (PDF)

■ AUTHOR INFORMATION

Corresponding Author

Kai-Hong Zhao − *State Key Laboratory of Agricultural Microbiology, Huazhong Agricultural University, Wuhan 430070, P.R. China;* orcid.org/0000-0003-1637-6187; Email: khzhao@163.com

Authors

Zi-Zhu Tan − *State Key Laboratory of Agricultural Microbiology, Huazhong Agricultural University, Wuhan 430070, P.R. China*

Xiao-Dan Li − *State Key Laboratory of Agricultural Microbiology, Huazhong Agricultural University, Wuhan 430070, P.R. China*

Chao-Di Kong − *State Key Laboratory of Agricultural Microbiology, Huazhong Agricultural University, Wuhan 430070, P.R. China*

Na Sha − *State Key Laboratory of Agricultural Microbiology, Huazhong Agricultural University, Wuhan 430070, P.R. China*

Ya-Nan Hou − *State Key Laboratory of Agricultural Microbiology, Huazhong Agricultural University, Wuhan 430070, P.R. China*

Complete contact information is available at: https://pubs.acs.org/10.1021/acssensors.0c02482

Author Contributions

Z.-Z.T. and X.-D.L. constructed the bacterial plasmids for the gene circle and performed the deletion of *hemF* in *E. coli*. Z.-Z.T., X.-D.L., C.-D.K., N.S., and Y.-N.H. carried out the experiment of heme or blood detection in vitro. Z.-Z.T. and X.-D.L. performed the bleeding detection in zebrafish. K.-H.Z. oversaw the design of experiments. K.-H.Z. and Z.-Z.T. analyzed the data and wrote the manuscript.

Notes

The authors declare no competing financial interest.

■ ACKNOWLEDGMENTS

K.-H.Z. are grateful for support (grants 31861143029 and 31770822) by the National Natural Science Foundation of China.

■ REFERENCES

(1) Claesen, J.; Fischbach, M. A. Synthetic Microbes As Drug Delivery Systems. *ACS Synth. Biol.* **2015**, *4*, 358−364.

(2) Danino, T.; Prindle, A.; Kwong, G. A.; Skalak, M.; Li, H.; Allen, K.; Hasty, J.; Bhatia, S. N. Programmable probiotics for detection of cancer in urine. *Sci. Transl. Med.* **2015**, *7*, 289ra84.

(3) Chen, Z.; Guo, L.; Zhang, Y.; Walzem, R.; Printz, R. L.; Morris, L. C.; Matafonova, E.; Stien, X.; Kang, L.; Coulon, D.; McGuinness, O. P.; Niswender, K. D.; Davies, S. S.; Davies, S. S. Incorporation of therapeutically modified bacteria into gut microbiota inhibits obesity. *J. Clin. Invest.* **2014**, *124*, 3391−3406.

(4) Olson, C. A.; Vuong, H. E.; Yano, J. M.; Liang, Q. Y.; Nusbaum, D. J.; Hsiao, E. Y. The Gut Microbiota Mediates the Anti-Seizure Effects of the Ketogenic Diet. *Cell* **2018**, *173*, 1728−1741.

(5) Riglar, D. T.; Giessen, T. W.; Baym, M.; Kerns, S. J.; Niederhuber, M. J.; Bronson, R. T.; Kotula, J. W.; Gerber, G. K.; Way, J. C.; Silver, P. A. Engineered bacteria can function in the mammalian gut long-term as live diagnostics of inflammation. *Nat. Biotechnol.* **2017**, *35*, 653−658.

(6) Archer, E. J.; Robinson, A. B.; Süel, G. M. Engineered E. coli That Detect and Respond to Gut Inflammation through Nitric Oxide Sensing. *ACS Synth. Biol.* **2012**, *1*, 451−457.

(7) Daeffler, K. N. M.; Galley, J. D.; Sheth, R. U.; Ortiz-Velez, L. C.; Bibb, C. O.; Shroyer, N. F.; Britton, R. A.; Tabor, J. J. Engineering bacterial thiosulfate and tetrathionate sensors for detecting gut inflammation. *Mol. Syst. Biol.* **2017**, *13*, 923.

(8) Levskaya, A.; Chevalier, A. A.; Tabor, J. J.; Simpson, Z. B.; Lavery, L. A.; Levy, M.; Davidson, E. A.; Scouras, A.; Ellington, A. D.; Marcotte, E. M.; Voigt, C. A. Engineering Escherichia coli to see light. *Nature* **2005**, *438*, 441−442.

(9) Schmidl, S. R.; Ekness, F.; Sofjan, K.; Daeffler, K. N.-M.; Brink, K. R.; Landry, B. P.; Gerhardt, K. P.; Dyulgyarov, N.; Sheth, R. U.; Tabor, J. J. Rewiring bacterial two-component systems by modular DNA-binding domain swapping. *Nat. Chem. Biol.* **2019**, *15*, 690−698.

(10) Carpenter, A.; Paulsen, I.; Williams, T. Blueprints for Biosensors: Design, Limitations, and Applications. *Genes* **2018**, *9*, 375.

(11) Mimee, M.; Nadeau, P.; Hayward, A.; Carim, S.; Flanagan, S.; Jerger, L.; Collins, J.; McDonnell, S.; Swartwout, R.; Citorik, R. J.; Bulović, V.; Langer, R.; Traverso, G.; Chandrakasan, A. P.; Lu, T. K. An ingestible bacterial-electronic system to monitor gastrointestinal health. *Science* **2018**, *360*, 915−918.

(12) Fu, Y.; Zhang, W.; Mandal, M.; Meng, M. Q.-H. Computer-Aided Bleeding Detection in WCE Video. *IEEE J. Biomed. Health.* **2014**, *18*, 636−642.

(13) Hassan, A. R.; Haque, M. A. Computer-aided gastrointestinal hemorrhage detection in wireless capsule endoscopy videos. *Comput. Methods Progr. Biomed.* **2015**, *122*, 341−353.

(14) Pogorelov, K.; Suman, S.; Azmadi Hussin, F.; Saeed Malik, A.; Ostroukhova, O.; Riegler, M.; Halvorsen, P.; Hooi Ho, S.; Goh, K. L. Bleeding detection in wireless capsule endoscopy videos - Color versus texture features. *J. Appl. Clin. Med. Phys.* **2019**, *20*, 141−154.

(15) Nemiroski, A.; Ryou, M.; Thompson, C. C.; Westervelt, R. M. Swallowable fluorometric capsule for wireless triage of gastrointestinal bleeding. *Lab Chip* **2015**, *15*, 4479−4487.

(16) Tsien, R. Y. Constructing and Exploiting the Fluorescent Protein Paintbox (Nobel Lecture). *Angew. Chem., Int. Ed.* **2009**, *48*, 5612−5626.

(17) Merzlyak, E. M.; Goedhart, J.; Shcherbo, D.; Bulina, M. E.; Shcheglov, A. S.; Fradkov, A. F.; Gaintzeva, A.; Lukyanov, K. A.; Lukyanov, S.; Gadella, T. W. J.; Chudakov, D. M. Bright monomeric red fluorescent protein with an extended fluorescence lifetime. *Nat. Methods* **2007**, *4*, 555−557.

(18) Murakoshi, H.; Lee, S.-J.; Yasuda, R. Highly sensitive and quantitative FRET−FLIM imaging in single dendritic spines using improved non-radiative YFP. *Brain Cell Biol.* **2008**, *36*, 31−42.

(19) Lee, J. H.; Kim, J.; Park, J. H.; Heo, W. D.; Lee, G. M. Analysis of Golgi pH in Chinese hamster ovary cells using ratiometric pH-sensitive fluorescent proteins. *Biotechnol. Bioeng.* **2019**, *116*, 1006−1016.

(20) Chen, Y.; Song, X.; Ye, S.; Miao, L.; Zhu, Y.; Zhang, R.-G.; Ji, G. Structural insight into enhanced calcium indicator GCaMP3 and GCaMPJ to promote further improvement. *Protein Cell* **2013**, *4*, 299−309.
(21) Bajar, B. T.; Lam, A. J.; Badiee, R. K.; Oh, Y.-H.; Chu, J.; Zhou, X. X.; Kim, N.; Kim, B. B.; Chung, M.; Yablonovitch, A. L.; Cruz, B. F.; Kulalert, K.; Tao, J. J.; Meyer, T.; Su, X.-D.; Lin, M. Z. Fluorescent indicators for simultaneous reporting of all four cell cycle phases. *Nat. Methods* **2016**, *13*, 993−996.
(22) Shu, X.; Royant, A.; Lin, M. Z.; Aguilera, T. A.; Lev-Ram, V.; Steinbach, P. A.; Tsien, R. Y. Mammalian expression of infrared fluorescent proteins engineered from a bacterial phytochrome. *Science* **2009**, *324*, 804−807.
(23) Li, X.-D.; Tan, Z.-Z.; Ding, W.-L.; Hou, Y.-N.; Kong, C.-D.; Zhao, B.-Q.; Zhao, K.-H. Design of small monomeric and highly bright near-infrared fluorescent proteins. *Biochim. Biophys. Acta* **2019**, *1866*, 1608−1617.
(24) Shcherbakova, D. M.; Verkhusha, V. V. Near-infrared fluorescent proteins for multicolor in vivo imaging. *Nat. Methods* **2013**, *10*, 751−754.
(25) Shemetov, A. A.; Oliinyk, O. S.; Verkhusha, V. V. How to Increase Brightness of Near-Infrared Fluorescent Proteins in Mammalian Cells. *Cell Chem. Biol.* **2017**, *24*, 758−766.
(26) Cummins, G.; Cox, B. F.; Ciuti, G.; Anbarasan, T.; Desmulliez, M. P. Y.; Cochran, S.; Steele, R.; Plevris, J. N.; Koulaouzidis, A. Gastrointestinal diagnosis using non-white light imaging capsule endoscopy. *Nat. Rev. Gastroenterol. Hepatol.* **2019**, *16*, 429−447.
(27) Sambrook, J.; Fritsch, E.; Maniatis, T. *Molecular Cloning: A Laboratory Manual*, 2nd ed.; Cold Spring Harbour Laboratory Press: New York, 1989.
(28) Zhang, J.; Wu, X.-J.; Wang, Z.-B.; Chen, Y.; Wang, X.; Zhou, M.; Scheer, H.; Zhao, K.-H. Fused-gene approach to photoswitchable and fluorescent biliproteins. *Angew. Chem., Int. Ed.* **2010**, *49*, 5456−5458.
(29) Ding, W.-L.; Hou, Y.-N.; Tan, Z.-Z.; Jiang, S.-P.; Miao, D.; Losi, A.; Gärtner, W.; Scheer, H.; Zhao, K.-H. Far-red acclimating cyanobacterium as versatile source for bright fluorescent biomarkers. *Biochim. Biophys. Acta* **2018**, *1865*, 1649−1656.
(30) Oh, J.-Y.; Hamm, J.; Xu, X.; Genschmer, K.; Zhong, M.; Lebensburger, J.; Marques, M. B.; Kerby, J. D.; Pittet, J.-F.; Gaggar, A.; Patel, R. P. Absorbance and redox based approaches for measuring free heme and free hemoglobin in biological matrices. *Redox Biol.* **2016**, *9*, 167−177.
(31) Niv, Y.; Battler, A.; Abuksis, G.; Gal, E.; Sapoznikov, B.; Vilkin, A. Endoscopy in Asymptomatic Minidose Aspirin Consumers. *Dig. Dis. Sci.* **2005**, *50*, 78−80.
(32) Ponka, P. Cell Biology of Heme. *Am. J. Med. Sci.* **1999**, *318*, 241−256.
(33) Layer, G.; Reichelt, J.; Jahn, D.; Heinz, D. W. Structure and function of enzymes in heme biosynthesis. *Protein Sci.* **2010**, *19*, 1137−1161.
(34) Breckau, D.; Mahlitz, E.; Sauerwald, A.; Layer, G.; Jahn, D. Oxygen-dependent coproporphyrinogen III oxidase (HemF) from Escherichia coli is stimulated by manganese. *J. Biol. Chem.* **2003**, *278*, 46625−46631.
(35) Ji, X.; Mo, T.; Liu, W. Q.; Ding, W.; Deng, Z.; Zhang, Q. Revisiting the Mechanism of the Anaerobic Coproporphyrinogen III Oxidase HemN. *Angew. Chem., Int. Ed.* **2019**, *58*, 6235−6238.
(36) Ding, W.-L.; Miao, D.; Hou, Y.-N.; Jiang, S.-P.; Zhao, B.-Q.; Zhou, M.; Scheer, H.; Zhao, K.-H. Small monomeric and highly stable near-infrared fluorescent markers derived from the thermophilic phycobiliprotein. ApcF2. *Biochim. Biophys. Acta* **2017**, *1864*, 1877−1886.
(37) Datsenko, K. A.; Wanner, B. L. One-step inactivation of chromosomal genes in Escherichia coli K-12 using PCR products. *Proc. Natl. Acad. Sci. U.S.A.* **2000**, *97*, 6640−6645.
(38) Xu, Q.-Z.; Han, J.-X.; Tang, Q.-Y.; Ding, W.-L.; Miao, D.; Zhou, M.; Scheer, H.; Zhao, K.-H. Far-red light photoacclimation: Chromophorylation of FR induced α- and β-subunits of allophycocyanin from Chroococcidiopsis thermalis sp. PCC7203. *Biochim. Biophys. Acta* **2016**, *1857*, 1607−1616.
(39) Torres, A. G.; Payne, S. M. Haem iron-transport system in enterohaemorrhagic Escherichia coli O157:H7. *Mol. Microbiol.* **1997**, *23*, 825−833.
(40) Berlec, A.; Štrukelj, B. A high-throughput biliverdin assay using infrared fluorescence. *J. Vet. Diagn. Invest.* **2014**, *26*, 521−526.
(41) Goldsmith, P. Zebrafish as a pharmacological tool: the how, why and when. *Curr. Opin. Pharmacol.* **2004**, *4*, 504−512.
(42) Yuan, G.; Wang, Y.; Yuan, X.; Zhang, T.; Zhao, J.; Huang, L.; Peng, S. T-2 toxin induces developmental toxicity and apoptosis in zebrafish embryos. *J. Environ. Sci.* **2014**, *26*, 917−925.
(43) Kelly, J. P.; Kaufman, D. W.; Jurgelon, J. M.; Sheehan, J.; Koff, R. S.; Shapiro, S. Risk of aspirin-associated major upper-gastrointestinal bleeding with enteric-coated or buffered product. *Lancet* **1996**, *348*, 1413−1416.
(44) Chang, K.; Bai, H. X.; Zhou, H.; Su, C.; Bi, W. L.; Agbodza, E.; Kavouridis, V. K.; Senders, J. T.; Boaro, A.; Beers, A.; Zhang, B.; Capellini, A.; Liao, W.; Shen, Q.; Li, X.; Xiao, B.; Cryan, J.; Ramkissoon, S.; Ramkissoon, L.; Ligon, K.; Wen, P. Y.; Bindra, R. S.; Woo, J.; Arnaout, O.; Gerstner, E. R.; Zhang, P. J.; Rosen, B. R.; Yang, L.; Huang, R. Y.; Kalpathy-Cramer, J. Residual Convolutional Neural Network for the Determination of IDH Status in Low- and High-Grade Gliomas from MR Imaging. *Clin. Cancer Res.* **2018**, *24*, 1073−1081.
(45) Chaudhary, K.; Poirion, O. B.; Lu, L.; Garmire, L. X. Deep Learning-Based Multi-Omics Integration Robustly Predicts Survival in Liver Cancer. *Clin. Cancer Res.* **2018**, *24*, 1248−1259.
(46) Rumelhart, D. E.; Hinton, G. E.; Williams, R. J. Learning representations by back-propagating errors. *Nature* **1986**, *323*, 533−536.
(47) Chollet, F. *Deep Learning with Python*; Manning: New York, 2018.
(48) Chen, X.; Xun, D.; Zheng, R.; Zhao, L.; Lu, Y.; Huang, J.; Wang, R.; Wang, Y. Deep-Learning-Assisted Assessment of DNA Damage Based on Foci Images and Its Application in High-Content Screening of Lead Compounds. *Anal. Chem.* **2020**, *15*, 14267−14277.
(49) Rogers, J. K.; Guzman, C. D.; Taylor, N. D.; Raman, S.; Anderson, K.; Church, G. M. Synthetic biosensors for precise gene control and real-time monitoring of metabolites. *Nucleic Acids Res.* **2015**, *43*, 7648−7660.
(50) Lutz, R.; Bujard, H. Independent and tight regulation of transcriptional units in Escherichia coli via the LacR/O, the TetR/O and AraC/I1-I2 regulatory elements. *Nucleic Acids Res.* **1997**, *25*, 1203−1210.
(51) Davidson, E. A.; Basu, A. S.; Bayer, T. S. Programming Microbes Using Pulse Width Modulation of Optical Signals. *J. Mol. Biol.* **2013**, *425*, 4161−4166.
(52) Castillo-Hair, S. M.; Baerman, E. A.; Fujita, M.; Igoshin, O. A.; Tabor, J. J. Optogenetic control of Bacillus subtilis gene expression. *Nat. Commun.* **2019**, *10*, 3099.
(53) Hensel, M.; Hinsley, A. P.; Nikolaus, T.; Sawers, G.; Berks, B. C. The genetic basis of tetrathionate respiration in Salmonella typhimurium. *Mol. Microbiol.* **1999**, *32*, 275−287.
(54) Williams, T. C.; Pretorius, I. S.; Paulsen, I. T. Synthetic Evolution of Metabolic Productivity Using Biosensors. *Trends Biotechnol.* **2016**, *34*, 371−381.
(55) Demosthenous, P.; Pitris, C.; Georgiou, J. Infrared Fluorescence-Based Cancer Screening Capsule for the Small Intestine. *IEEE Trans. Biomed. Circuits Syst.* **2016**, *10*, 467−476.
(56) Gorman, S.; Fox, D. T.; Wahl, G. M. Recombinase-mediated gene activation and site-specific integration in mammalian cells. *Science* **1991**, *251*, 1351−1355.
(57) Kotula, J. W.; Kerns, S. J.; Shaket, L. A.; Siraj, L.; Collins, J. J.; Way, J. C.; Silver, P. A. Programmable bacteria detect and record an environmental signal in the mammalian gut. *Proc. Natl. Acad. Sci. U.S.A.* **2014**, *111*, 4838−4843.

https://doi.org/10.1021/acssensors.0c02482
ACS Sens. 2021, 6, 1770−1778

(58) Kumagai, A.; Ando, R.; Miyatake, H.; Greimel, P.; Kobayashi, T.; Hirabayashi, Y.; Shimogori, T.; Miyawaki, A. A Bilirubin-Inducible Fluorescent Protein from Eel Muscle. *Cell* **2013**, *153*, 1602−1611.
(59) Wennberg, R. P.; Ahlfors, C. E.; Bhutani, V. K.; Johnson, L. H.; Shapiro, S. M. Toward Understanding Kernicterus: A Challenge to Improve the Management of Jaundiced Newborns. *Pediatrics* **2006**, *117*, 474−485.

https://doi.org/10.1021/acssensors.0c02482
ACS Sens. 2021, 6, 1770−1778